Understanding Cation dynamics in Caesium Substituted Organohalide Perovskites

Contact *Artem Bakulin (a.bakulin@imperial.ac.uk)*

N. P. Gallop

Dept. of Chemistry – Imperial College London
Molecular Sciences Research Hub
83 Wood Lane, London W12 0BZ

J. Ye

Dept. of Materials – Imperial College London
Royal School of Mines, London SW7 2AZ

G. Greetham

Central Laser Facility, Rutherford Appleton Laboratory
Harwell Campus, Didcot, OX11 0QX

R Hoye

Dept. of Materials – Imperial College London
Royal School of Mines, London SW7 2AZ

A. A. Bakulin

Dept. of Chemistry – Imperial College London
Molecular Sciences Research Hub
83 Wood Lane, London W12 0BZ

Introduction

Organohalide perovskites (OHPs) are presently enjoying considerable academic and industrial interest[1–3]. Since their first use as light harvesting materials. in 2009, their photovoltaic power conversion efficiencies of perovskite photovoltaics have climbed as high as 25%[4] (as of May 2020), the highest of any emerging PV technology. These record efficiencies, combined with their ease and low cost of production, broad material tuneability, and potential use in flexible PV modules, have resulted in an explosion in research[1], in applications as diverse as thermoelectric materials[5], LEDs[1,6,7] and lasers[8], and as media for nonvolatile memory[9]. Consequently, developing a comprehensive understanding of their macroscopic and microscopic behaviours is essential. In particular, OHPs, typically feature an organic cation within the crystal lattice[10]. As can be seen in Fig. 1, an inorganic lattice—consisting of covalently bound PbX_3 octahedra (here, X refers to any combination of halide ions)—creates a 'cage', whose cavity is occupied by the organic (or occasionally in the case of perovskite photovoltaics, an inorganic) *A-site* cation. Interestingly, the organic cations have been shown to be highly rotationally mobile at conditions relevant to device operation. Unsurprisingly, this has sparked considerable interest as researchers aim to develop a comprehensive understanding of the molecular origins of the remarkable optoelectronic properties of OHPs[11–14]. As such, the rotational properties of the A-site cations have been extensively studied using a battery of experimental techniques, including steady state IR[15] and millimeter wave[16] spectroscopy, calorimetry[15], solid-state NMR[17–19], neutron scattering[20–22], and most recently time-resolved ultrafast spectroscopy[10,14,23–25].

From these extensive investigations, a picture of the rotational dynamics of the A-site cation within OHPs has emerged. In the case of the common organic cation methylammonium (MA) two regimes of rotational motion exist: a rapid (but low angle) 'wobbling in a cone' motion, and a large angle (but slower) thermally activated reorientational 'jump'[10,14,23,24] between adjacent equilibrium positions. These 'wobble' and 'jump' timescales dominate at timescales of 300—600 ps, and >2 ps respectively. Conversely, for the popular inorganic cation formamidinium (FA), the lack of axial symmetry means that whilst coexisting fast and slow rotational processes occur, they cannot be easily ascribed to a single rotational mode[22,25]. Regardless of the A-site species however, these rotational dynamics have been found to be highly sensitive to the chemical

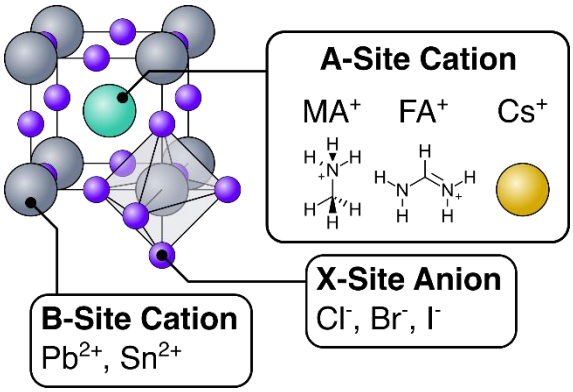

Figure 1 Generalized crystal structure of a metal-halide perovskite

structure, phase, and other factors intrinsic to the material. Studies on mixed-halide perovskites have found that partial substitution of the X-site anions results in a substantial slowdown in the rotational dynamics of the MA ion and has been ascribed to the formation of an anisotropic potential within the octahedral cavity. Here, the potential anisotropy can be understood as arising from variations in the hydrogen bonds between the ammonium group of MA, and the halide ions themselves. However, it has been noted that such a static picture would severely underestimate the ease with which organic cations rotate within OHPs[10]. An alternative (and potentially complementary) explanation has been put forward, in which the PbX_3 phonon frequencies—which will change with differing halide composition—dictate the rotational mobility of the cation. Here, the dynamic fluctuations in the PbX_3 lattice are understood as modulating the energy barriers between adjacent equilibrium sites, in a way that provides the organic cation with 'windows of opportunity' in which they can reorient themselves. Understanding the interplay of these two effects is essential to developing a more unified model of cation dynamics in MHPs.

To this end, we made use of the facilities of the LIFETime experimental setup at the Central Laser Facility to study the rotational dynamics of four MHPs: $MAPbI_3$, $MA_{0.9}Cs_{0.1}PbI_3$, $MA_{0.8}Cs_{0.2}PbI_3$, and $MA_{0.7}Cs_{0.3}PbI_3$. More specifically, we utilized the 2DIR capabilities of the LIFETime setup, to obtain the time-resolved rotational anisotropy curves for our four samples. This approach has been reported extensively elsewhere within the literature[10,24–26]. Briefly, the sample is pumped with a

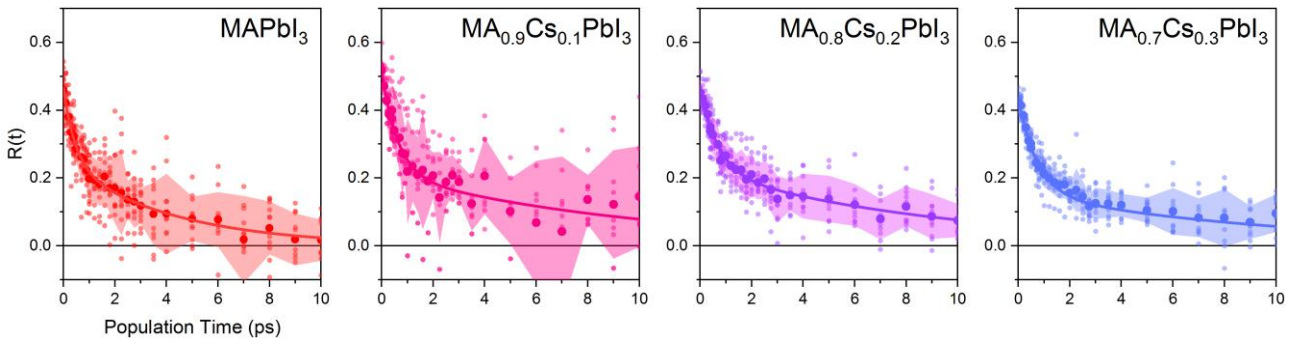

Figure 2 Rotational anisotropy decays of $MA_xCs_{1-x}PbI_3$ (x = 0.0—0.3). The solid points represent averages across all runs (semitranspatent points), whilst the solid lines represent a fit of this data using Eqn. 2. The shaded region denotes the standard error of the measurements.

Linearly polarized IR pulse resonant with the ~1470 cm^{-1} N-H stretching mode of methylammonium, whose vibrational transition dipole moment is collinear with the C-N bond of the molecule. Because absorption is related to the angle formed by the pump field and the transition dipole of the cation, the pump pulse selects a sub ensemble of MA ions whose C-N axes are oriented in a common direction. As time goes on, the rotation of the organic cation will cause their dipoles to become scrambled, which may be monitored *via* a set of probe IR pulses whose polarizations are either parallel or orthogonal to that of the pump. This enables the time-dependent rotational anisotropy of the material to be sampled as:

$$\boldsymbol{R(t)} = \frac{\Delta\boldsymbol{\alpha}_{\parallel} - \Delta\boldsymbol{\alpha}_{\perp}}{\Delta\boldsymbol{\alpha}_{\parallel} + 2\Delta\boldsymbol{\alpha}_{\perp}} \qquad \textbf{(1)}$$

Where $\boldsymbol{R(t)}$ is the rotational anisotropy, and $\Delta\boldsymbol{\alpha}_{\parallel}$ and $\Delta\boldsymbol{\alpha}_{\perp}$ represent the pump-induced absorbance change for the parallel and orthogonally polarized probe pulse, respectively. R(t) will typically start from a value of 0.4 (all cations aligned along a common direction), and decay over time as their rotational orientations become scrambled. The resulting curves for the four samples are given in Fig. 2. In each case, between 7 and 10 averages were taken at different points across two separately fabricated films. Differences in the films' surface characteristics result in varying levels of scattering, and thus variation in the uncertainty in each set of 2DIR traces. Nevertheless, significant differences in their rotational dynamics can be seen across the series. For example, for $MAPbI_3$ (i.e.: no caesium addition), the transient anisotropy response has effectively decayed to 0 within the total measurement time, whilst in the same time, the transient anisotropy decays of all other perovskites have only decreased by approximately 75%. To quantify these timescales, we fit the anisotropy decays using the following model[24,26]:

$$\boldsymbol{R(t)} = \frac{2}{5}\left[\boldsymbol{S^2 e^{-t/\tau_{jump}} + (1 - S^2) e^{t/\tau_{wob} - t/\tau_{jump}}}\right] \qquad \textbf{(2)}$$

Where $\boldsymbol{\tau_{jump}}$ and $\boldsymbol{\tau_{wob}}$ are respectively the timescales of the two rotational processes within the perovskite: a high-amplitude, low-frequency 'jump' between adjacent equilibrium positions, and a low-amplitude, high-frequency 'wobbling' within the equilibrium position, and $\boldsymbol{S}$ is a dimensionless constant related to the solid angle associated with the wobbling motion.

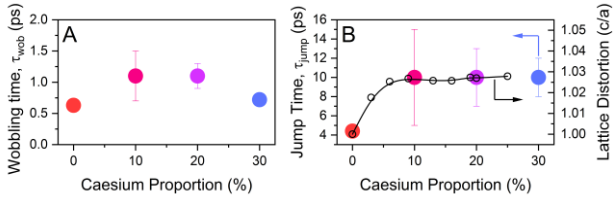

Figure 3 Extracted wobbling and jump time parameters, obtained by fitting the four anisotropy decays in Fig. 2 to Eqn. 2. The black line in (B) is digitally extracted from Ref. [27]

These extracted values of $\boldsymbol{\tau_{jump}}$ and $\boldsymbol{\tau_{wob}}$ are also plotted in Fig. 3.Whilst no significant trend is seen for $\boldsymbol{\tau_{wob}}$, interestingly, a more than 6 ps increase in $\boldsymbol{\tau_{jump}}$ occurs as the caesium content is increased from 0 to >10%. Also notable is the rapid saturation of this effect, with $\boldsymbol{\tau_{jump}}$ remaining constant (within the experimental uncertainty) for a caesium content of >10%. This is suggestive of a picture in which caesium inhibits the frequency of large amplitude reorientational jumps, whilst leaving the organic cations largely free to rattle around their local equilibrium positions.

We now consider the likely mechanisms behind this slowing of cation dynamics. Importantly, as the X-site ionic species remains unchanged across our chosen materials, we expect other effects besides hydrogen bonding to dictate their dynamics. A*b initio* studies by Ghosh *et al.* on $FA_xCs_{1-x}PbI_3$ suggest that the octahedral cavity distorts in response to caesium addition[27], whilst Raman studies on $MA_xCs_{1-x}PbI_3$ suggest that the inorganic cage rigidizes in response to caesium[28]. We also note that the trend in lattice distortion obtained by Ghosh *et al.* (black points/line in Fig. 3(B)) correlate extremely well with our observed trend in jump times, although we cannot necessarily rule out the nucleation of pure $CsPbI_3$ domains, which may prevent further caesium incorporation above substitution ratios of 10%[29]. Regardless, we believe that this octahedral cavity distortion, works in synergy with the rigidisation of the PbI_3 lattice—the distortions result in an anisotropic electrostatic potential that will favour certain cation orientations, whilst the rigidized lattice precludes modulations of the energetic barrier which would otherwise facilitate reorientation. Furthermore, we note that the (~6 ps) increase in jump time upon addition of 10% Cs is dramatic in comparison to previous reports, in which the X-site ions within the perovskite are substituted (1.5—1.8 ps)[24], further suggesting that, even if hydrogen bonding plays a role in dictating the dynamics of the organic cation, alterations to the octahedral cavity shape and flexibility are more significant. Most importantly, our results point towards an interplay between the static and dynamic disorder in these materials, which may have implications for their stability and optoelectronic performance in future.

Conclusions

In Conclusion, we utilized 2DIR spectroscopy to interrogate the rotational dynamics of caesium doped $MAPbI_3$. We find a 2.5-fold increase in the reorientation of the MA cation upon as little as 10% caesium addition. Comparison of our result with previously reported *ab initio* calculations and Raman studies implicate rigidisation of the inorganic lattice, coupled with distortion of the octahedral cavity as the underlying cause of this effect.

Acknowledgements

NPG and AAB gratefully acknowledge support from the ERC (Grant No. 639750) under their Horizon2020 framework. AAB is a Royal Society University Research Fellow. NPG and AAB thank Thomas LaCoeur Jansen for his continued work in support of this project.

References

(1) Stranks, S. D.; Snaith, H. J. Metal-Halide Perovskites for Photovoltaic and Light-Emitting Devices. *Nat. Nanotechnol.* **2015**, *10* (5), 391–402.

(2) Egger, D. A.; Bera, A.; Cahen, D.; Hodes, G.; Kirchartz, T.; Kronik, L.; Lovrincic, R.; Rappe, A. M.; Reichman, D. R.; Yaffe, O. What Remains Unexplained about the Properties of Halide Perovskites? *Adv. Mater.* **2018**, *30* (20), 1800691.

(3) Brenner, T. M.; Egger, D. A.; Kronik, L.; Hodes, G.; Cahen, D. Hybrid Organic - Inorganic Perovskites: Low-Cost Semiconductors with Intriguing Charge-Transport Properties. *Nature Reviews Materials*. Nature Publishing Group January 11, 2016, p 15007.

(4) Best Research-Cell Efficiency Chart | Photovoltaic Research | NREL https://www.nrel.gov/pv/cell-efficiency.html (accessed Oct 26, 2020).

(5) He, Y.; Galli, G. Perovskites for Solar Thermoelectric Applications: A First Principle Study of CH3NH3AI3 (A = Pb and Sn). *Chem. Mater.* **2014**, *26* (18), 5394–5400.

(6) Yantara, N.; Bhaumik, S.; Yan, F.; Sabba, D.; Dewi, H. A.; Mathews, N.; Boix, P. P.; Demir, H. V.; Mhaisalkar, S. Inorganic Halide Perovskites for Efficient Light-Emitting Diodes. *J. Phys. Chem. Lett.* **2015**, *6* (21), 4360–4364.

(7) Cho, H.; Jeong, S. H.; Park, M. H.; Kim, Y. H.; Wolf, C.; Lee, C. L.; Heo, J. H.; Sadhanala, A.; Myoung, N. S.; Yoo, S.; et al. Overcoming the Electroluminescence Efficiency Limitations of Perovskite Light-Emitting Diodes. *Science (80-.).* **2015**, *350* (6265), 1222–1225.

(8) Zhang, Q.; Su, R.; Du, W.; Liu, X.; Zhao, L.; Ha, S. T.; Xiong, Q. Advances in Small Perovskite-Based Lasers. *Small Methods* **2017**, *1* (9), 1700163.

(9) Liu, D.; Lin, Q.; Zang, Z.; Wang, M.; Wangyang, P.; Tang, X.; Zhou, M.; Hu, W. Flexible All-Inorganic Perovskite CsPbBr3 Nonvolatile Memory Device. *ACS Appl. Mater. Interfaces* **2017**, *9* (7), 6171–6176.

(10) Gallop, N. P.; Selig, O.; Giubertoni, G.; Bakker, H. J.; Rezus, Y. L. A.; Frost, J. M.; Jansen, T. L. C.; Lovrincic, R.; Bakulin, A. A. Rotational Cation Dynamics in Metal Halide Perovskites: Effect on Phonons and Material Properties. *J. Phys. Chem. Lett.* **2018**, *9* (20), 5987–5997.

(11) Gong, J.; Yang, M.; Ma, X.; Schaller, R. D.; Liu, G.; Kong, L.; Yang, Y.; Beard, M. C.; Lesslie, M.; Dai, Y.; et al. Electron-Rotor Interaction in Organic-Inorganic Lead Iodide Perovskites Discovered by Isotope Effects. *J. Phys. Chem. Lett.* **2016**, *7* (15), 2879–2887.

(12) Bonn, M.; Miyata, K.; Hendry, E.; Zhu, X. Y. Role of Dielectric Drag in Polaron Mobility in Lead Halide Perovskites. *ACS Energy Letters*. American Chemical Society November 10, 2017, pp 2555–2562.

(13) Zhu, X. Y.; Podzorov, V. Charge Carriers in Hybrid Organic-Inorganic Lead Halide Perovskites Might Be Protected as Large Polarons. *Journal of Physical Chemistry Letters*. American Chemical Society December 3, 2015, pp 4758–4761.

(14) Zhu, H.; Miyata, K.; Fu, Y.; Wang, J.; Joshi, P. P.; Niesner, D.; Williams, K. W.; Jin, S.; Zhu, X. Y. Screening in Crystalline Liquids Protects Energetic Carriers in Hybrid Perovskites. *Science (80-.).* **2016**, *353* (6306), 1409–1413.

(15) Onoda-Yamamuro, N.; Matsuo, T.; Suga, H. Calorimetric and IR Spectroscopic Studies of Phase Transitions in Methylammonium Trihalogenoplumbates (II)†. *J. Phys. Chem. Solids* **1990**, *51* (12), 1383–1395.

(16) Poglitsch, A.; Weber, D. Dynamic Disorder in Methylammoniumtrihalogenoplumbates (II) Observed by Millimeter-Wave Spectroscopy. *J. Chem. Phys.* **1987**, *87* (11), 6373–6378.

(17) Wasylishen, R. E.; Knop, O.; Macdonald, J. B. Cation Rotation in Methylammonium Lead Halides. *Solid State Commun.* **1985**, *56* (7), 581–582.

(18) Bernard, G. M.; Wasylishen, R. E.; Ratcliffe, C. I.; Terskikh, V.; Wu, Q.; Buriak, J. M.; Hauger, T. Methylammonium Cation Dynamics in Methylammonium Lead Halide Perovskites: A Solid-State NMR Perspective. *J. Phys. Chem. A* **2018**, *122* (6), 1560–1573.

(19) Kubicki, D. J.; Prochowicz, D.; Hofstetter, A.; Péchy, P.; Zakeeruddin, S. M.; Grätzel, M.; Emsley, L. Cation Dynamics in Mixed-Cation (MA)x(FA)1-XPbI3 Hybrid Perovskites from Solid-State NMR. *J. Am. Chem. Soc.* **2017**, *139* (29), 10055–10061.

(20) Leguy, A. M. A.; Frost, J. M.; McMahon, A. P.; Sakai, V. G.; Kochelmann, W.; Law, C.; Li, X.; Foglia, F.; Walsh, A.; O'Regan, B. C.; et al. The Dynamics of Methylammonium Ions in Hybrid Organic-Inorganic Perovskite Solar Cells. *Nat. Commun.* **2015**, *6* (1), 7124.

(21) Chen, T.; Foley, B. J.; Ipek, B.; Tyagi, M.; Copley, J. R. D.; Brown, C. M.; Choi, J. J.; Lee, S. H. Rotational Dynamics of Organic Cations in the CH3NH3PbI3 Perovskite. *Phys. Chem. Chem. Phys.* **2015**, *17* (46), 31278–31286.

(22) Fabini, D. H.; Siaw, T. A.; Stoumpos, C. C.; Laurita, G.; Olds, D.; Page, K.; Hu, J. G.; Kanatzidis, M. G.; Han, S.; Seshadri, R. Universal Dynamics of Molecular Reorientation in Hybrid Lead Iodide Perovskites. *J. Am. Chem. Soc.* **2017**, *139* (46), 16875–16884.

(23) Bakulin, A. A.; Selig, O.; Bakker, H. J.; Rezus, Y. L. A.; Müller, C.; Glaser, T.; Lovrincic, R.; Sun, Z.; Chen, Z.; Walsh, A.; et al. Real-Time Observation of Organic Cation Reorientation in Methylammonium Lead Iodide Perovskites. *J. Phys. Chem. Lett.* **2015**, *6* (18), 3663–3669.

(24) Selig, O.; Sadhanala, A.; Müller, C.; Lovrincic, R.; Chen, Z.; Rezus, Y. L. A.; Frost, J. M.; Jansen, T. L. C.; Bakulin, A. A. Organic Cation Rotation and Immobilization in Pure and Mixed Methylammonium Lead-Halide Perovskites. *J. Am. Chem. Soc.* **2017**, *139* (11), 4068–4074.

(25) Taylor, V. C. A.; Tiwari, D.; Duchi, M.; Donaldson, P. M.; Clark, I. P.; Fermin, D. J.; Oliver, T. A. A. Investigating the Role of the Organic Cation in Formamidinium Lead Iodide Perovskite Using Ultrafast Spectroscopy. *J. Phys. Chem. Lett.* **2018**, *9* (4), 895–901.

(26) Bakulin, A. A.; Selig, O.; Bakker, H. J.; Rezus, Y. L. A.; Müller, C.; Glaser, T.; Lovrincic, R.; Sun, Z.; Chen, Z.; Walsh, A.; et al. Real-Time Observation of Organic Cation Reorientation in Methylammonium Lead Iodide Perovskites. *J. Phys. Chem. Lett.* **2015**, *6* (18), 3663–3669.

(27) Ghosh, D.; Walsh Atkins, P.; Islam, M. S.; Walker, A. B.; Eames, C. Good Vibrations: Locking of Octahedral Tilting in Mixed-Cation Iodide Perovskites for Solar Cells. *ACS Energy Lett.* **2017**, *2* (10), 2424–2429.

(28) Damle, V. H.; Gouda, L.; Tirosh, S.; Tischler, Y. R. Structural Characterization and Room Temperature Low-Frequency Raman Scattering from MAPbI3 Halide Perovskite Films Rigidized by Cesium Incorporation. *ACS Appl. Energy Mater.* **2018**, *1* (12), 6707–6713.

(29) Niemann, R. G.; Kontos, A. G.; Palles, D.; Kamitsos, E. I.; Kaltzoglou, A.; Brivio, F.; Falaras, P.; Cameron, P. J. Halogen Effects on Ordering and Bonding of CH3NH3+ in CH3NH3PbX3 (X = Cl, Br, I) Hybrid Perovskites: A Vibrational Spectroscopic Study. *J. Phys. Chem. C* **2016**, *120* (5), 2509–2519.